Gamma-ray studies in ^{45}V

S. A. Gronemeyer,* L. Meyer-Schützmeister, and A. J. Elwyn
Argonne National Laboratory, Argonne, Illinois 60439

G. Hardie
Argonne National Laboratory, Argonne, Illinois 60439
and Western Michigan University, Kalamazoo, Michigan 49008

(Received 2 October 1979)

The level scheme of ^{45}V was studied with the reaction $^{40}Ca(^{7}Li,2n)^{45}V$ using ^{7}Li beams of 14–16-MeV energies. Prompt and delayed n-γ and γ-γ coincidences revealed a doublet at an excitation energy of about 57 keV with a separation energy of only 800 eV. The half-life of the upper member, a $3/2^-$ state, was measured to be 430 ± 80 nsec. This state decays strongly via internal conversion to the lower member of the doublet, a $5/2^-$ state. The half-life of the latter level was measured to be $\lesssim 4.2$ nsec. Since ^{45}V is a $T = 1/2$ nucleus and the mirror of the well-known ^{45}Ti nucleus, Coulomb displacement energies could be deduced. A comparison of these Coulomb displacement energies with those of neighboring nuclei, the measured lifetimes, and the observed γ-γ and n-γ prompt and delayed coincidence spectra established nearly all the ^{45}V levels expected below the proton separation energy of 1.62 MeV, namely, $7/2^-$(g.s.), $5/2^-$(56.4 keV), $3/2^-$(57.2 keV), $3/2^+$(386.1 keV), $5/2^+$(796.8 keV), and $7/2^+$(1273 keV). The expected four highest bound levels, in particular the $9/2^-$ and $11/2^-$ states, are not seen in the present experiment. The latter two states are supposed to decay either completely or predominantly to the ground state and hence are not observable in these γ-γ coincidence studies. The third and fourth levels were not seen in ^{45}Ti γ-ray spectra which exhibit much higher counting rates than those of ^{45}V. They are therefore not expected to be observable in the present ^{45}V spectra. ^{45}V gamma rays were also seen in the $^{40}Ca(^{6}Li,n)^{45}V$ reaction with a 10- and a 13.5-MeV ^{6}Li beam. This reaction has a smaller production cross section and is therefore less suited for detailed studies.

NUCLEAR REACTIONS $^{40}Ca(^{7}Li,2n)^{45}V$: singles spectra, prompt and delayed n-γ and γ-γ coincidences with $E_{^7Li} = 14,\ 15,\ 16$ MeV. $^{40}Ca(^{6}Li,n)^{45}V$ with 10, 13.5 MeV ^{6}Li: n-γ and γ-γ coincidences. Measurement of $T_{1/2} = 430 \pm 80$ nsec for the 57.2-keV state and ≤ 4.2 nsec for the 56.4-keV state. Deduced $\frac{7}{2}^-$(g.s.); $\frac{5}{2}^-$(56.4); $\frac{3}{2}^-$(57.2); $\frac{3}{2}^+$(386.1); $\frac{5}{2}^+$(796.8); $\frac{7}{2}^+$(1273), and γ decay of these states.

I. INTRODUCTION

The study of nuclear properties in ^{45}V is of special importance since it is a $T=\frac{1}{2}$ nucleus and the mirror of the well-studied[1] nucleus ^{45}Ti. The knowledge of its level scheme and spin assignments offers the possibility to extract Coulomb displacement energies of negative as well as positive-parity states. These Coulomb shifts are not constant, but vary, thus indicating charge-dependent effects which change for the different states. They provide the means to study nuclear structure and nucleon-nucleon interactions in more detail.

It has been observed[2] that in $T=\frac{1}{2}$ mirror nuclei of the $f_{7/2}$ shell with mass $A = 4n+3$, the Coulomb interaction of a $d_{3/2}$ proton hole and an $f_{7/2}$ valence proton shows an A dependence; one might ask if this dependence holds also for nuclei with $A = 4n+1$, a group to which the pair ^{45}Ti–^{45}V belongs. So far very little is known of ^{45}V. The only data available are those reported by Mueller *et al.*[3] These authors have been able to determine the mass of the ground state and to observe a state at an excitation energy of 0.39 MeV by using the reaction $^{50}Cr(p, ^{6}He)^{45}V$.

^{45}V has a small production cross section for various combinations of target and projectile nuclei–much smaller than those of competing reactions. This fact makes angular correlation, and even angular distribution, measurements in γ-ray studies hard or impossible. For this reason our investigations consisted mainly of prompt and delayed coincidence studies using neutron, x-ray, and γ-ray detectors.

Only a few bound levels are expected in ^{45}V because of its low particle separation energy of 1.62 MeV. Most of these levels should be observable. It might also be possible, according to ^{45}Ti, to observe one or two states whose lifetimes one can measure by delayed coincidence experiments. Such results in combination with the known level scheme of ^{45}Ti should permit us to make spin and parity assignments and extract Coulomb shifts. The latter are expected to show regularities which not only should confirm the adopted spin assignments but also will be compared with those of neighboring $T=\frac{1}{2}$ nuclear pairs.

II. EXPERIMENTAL PROCEDURE

The small production cross sections of ^{45}V, which are predicted by evaporation theories, make it necessary to use large acceptance angles for the detector system. Since in particular most ^{45}V γ rays were only observable in coincidence experiments a flat target chamber was used which permitted us to place two detectors at 90° to the beam direction with a closest distance from the target spot of ≤ 1 cm. The target was positioned at an angle of 45° to the beam. It was a rolled self-supported and enriched (>99.99%) ^{40}Ca foil which contained less than 0.01% ^{42}Ca. γ rays with energies larger than 120 keV were measured with Li-drifted Ge detectors (volume ≈ 80 cm^3), referred to as γ-detector, and γ rays with energies less than 120 keV by an x-ray detector (x-detector) which consisted of an intrinsic Ge detector with a sensitive volume of about 12.5 cm^3. Neutrons and γ rays were registered and separated by pulse shape discrimination in a 5 cm diameter by 2.5 cm thick stilbene crystal. They are referred to by n and "γ."

Singles γ-ray spectra were measured with the γ detectors and the x-ray detector displaying energies from 20 to about 4000 keV. Prompt and delayed coincident events were studied in the following detector combinations: γ-γ, γ-x, n-x, and "γ"-x. As in earlier work,[4] in each case a coincidence was measured as a three-parameter event consisting either of two coinciding photon pulses or a neutron and a coinciding photon pulse and the time difference between them. Since in the present studies ^{45}V is formed by neutron emission from the compound nucleus, the start of the coincident event for the n-x experiment is determined by the signal from the stilbene detector and the stop pulse by the x-detector. In γ-x coincidences, however, the start pulse is obtained from the γ detector and the stop pulse from the x-detector since ^{45}V γ rays with energies smaller than 100 keV might be emitted by isomeric states. For later detailed analysis, all data were recorded on magnetic tape.

III. SEARCH FOR ^{45}V GAMMA RAYS

Recently Brown *et al.*[5] calculated Coulomb displacement energies of analog states in $f_{7/2}$ nuclei which have a $(f_{7/2})^n$ nucleon configuration. These calculations indicate that instead of the measured γ transition $\frac{5}{2}^- \rightarrow \frac{7}{2}^-$ (ground state) of 39.8-keV energy in ^{45}Ti a transition energy of 63 keV is expected in the mirror nucleus ^{45}V. Since in general the values predicted by Brown *et al.*[5] and those measured agree quite well (most differences are smaller than ± 15 keV), the study of ^{45}V decay started by searching for a γ ray of about 63-keV energy. In the first attempt ^{45}V was produced by the $^{40}Ca(^6Li,n)^{45}V$ reaction and a γ ray of 56.4-keV energy (instead of 63 keV) was observed; this seemed to be a candidate for the $\frac{5}{2}^- \rightarrow \frac{7}{2}^-$ transition in ^{45}V. However, its intensity was too small in comparison to those of other γ rays originating in competing reactions and coincidence measurements did not seem feasible for detailed studies. Evaporation calculations were performed using the code ALICE by Blann and Plasil[6] which showed that the production cross section of ^{45}V is expected to be larger in the $^{40}Ca(^7Li,2n)^{45}V$ reaction than in ^6Li bombardment of ^{40}Ca. The calculated cross section for various residual nuclei are presented in Fig. 1 for ^7Li beams with energies between 12 and 18 MeV. According to these calculations the production cross section of ^{45}V is rather constant over this ^7Li energy range and is about two orders of magnitude smaller than those of ^{45}Sc, ^{42}Ca, and the mirror nucleus ^{45}Ti, the

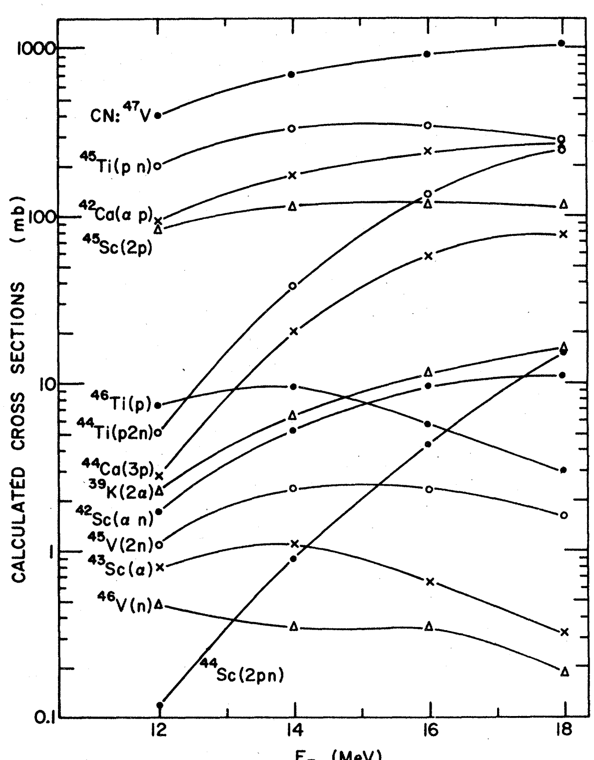

FIG. 1. Calculated production cross sections for various final nuclei emerging from the bombardment of ^{40}Ca with ^7Li beams of different energies. The calculations were performed using the computer code of Ref. 6. The evaporated particles are indicated in parentheses.

three nuclei most strongly populated. For a ^{7}Li beam of 16 MeV a singles γ-ray spectrum over the energy region of interest is presented in Fig. 2(a) using the intrinsic Ge detector (x-detector). Besides the Pb x-rays, this spectrum contains the low-energy γ rays of ^{45}Ti and ^{44}Sc. The 39.8-keV ^{45}Ti γ ray is much stronger than the one at 36.4-keV energy since the latter γ ray corresponds to an $E2$ transition with an internal conversion coefficient $\alpha = 16$, while the first one is an $M1$ transition and, assuming no $E2$ admixture, has $\alpha = 0.2$. The prospective 56.4-keV ^{45}V γ ray which has been seen in the ^{40}Ca(^{6}Li,n)^{45}V reaction is again present. Its intensity as expected from the calculations (Fig. 1) is much weaker than the 39.8-keV ^{45}Ti line. However, this γ ray should be enhanced in n-x coincidence experiments since many of the strong competing γ rays are produced with the emission of only one neutron (as in the nuclei ^{45}Ti and ^{44}Sc) or no neutron at all, while ^{45}V originates together with two neutrons (see Fig. 1). This is indeed observed in Figs. 2(b) and 2(c). They show the same γ-ray spectrum as Fig. 2(a) but now in coincidence with either a neutron [Fig. 2(c)] or a γ ray [Fig. 2(b)], both registered in the stilbene crystal and indicated by n and "γ," respectively. A coincidence event was recognized by a time-to-pulse-height converter which accepted an event within the time range of 0.5 μsec. Since the 36.4-keV ^{45}Ti γ ray has a long lifetime,[7] $T_{1/2} = 3.1$ μsec (very much greater than the 0.5 μsec time range), the yield of this γ ray is reduced in the coincidence measurements relative to the singles spectrum. Comparison of the two coincidence spectra exhibits two facts: (a) the signal-to-noise ratio is greatly enhanced in the n-x spectra, and (b) the intensity of the 56.4-keV γ ray increases in the n-x spectrum while that of the other γ rays decrease, as shown in Table I. Table I presents the yields and ratios for the various γ rays in the "γ"-x and n-x coincidence spectra, and indicates that the abundance of neutrons in the production of the 56.4-keV γ ray must be

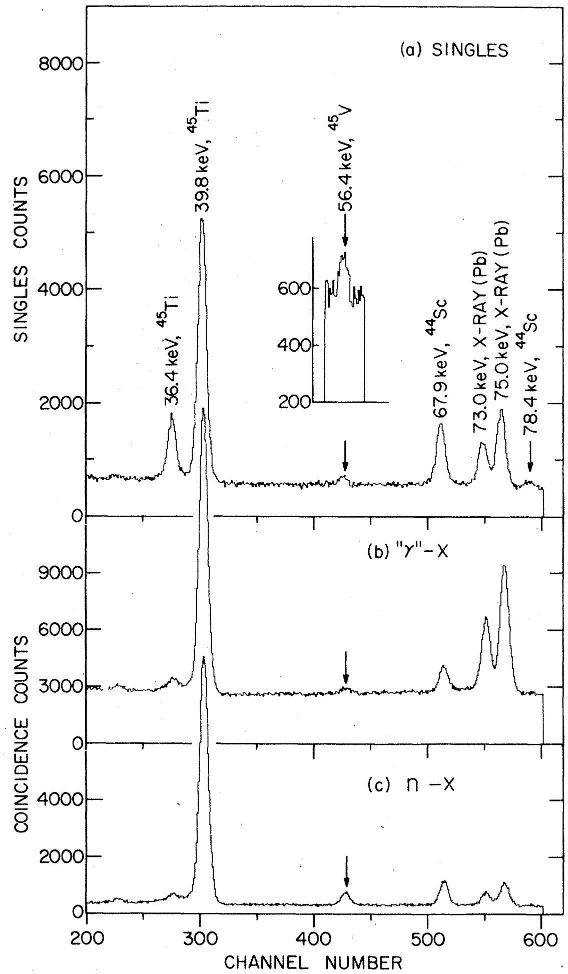

FIG. 2. Spectra of low-energy γ rays of ^{45}Ti, ^{44}Sc, and ^{45}V observed in the bombardment of ^{40}Ca with a 16-MeV ^{7}Li beam. The top spectra (a) is the singles x-spectrum, (b) the "γ"-x coincidence spectrum, and (c) n-x coincidence spectrum. x represents the γ-ray spectrum measured by the intrinsic Ge detector, and "γ" the γ spectrum registered with the stilbene crystal. Coincidences were accepted within the time range of 0.5 μsec. The energies indicated are those obtained in the present work.

TABLE I. Comparison of low-energy γ-ray yields measured in "γ"-x (yield Y_1) and n-x (yield Y_2) coincidence spectra.

	E_γ(keV) nucleus	36.4 ^{45}Ti	39.8 ^{45}Ti	56.4 ^{45}V	67.9 ^{44}Sc	73.0 x ray	75.0 x ray	78.4 ^{44}Sc
"γ"-x		7544	145 393	3722	11 898	35 479	66 089	679
n-x		4094	84 170	4551	7 915	3 849	7 841	450
Ratio =	Y_2/Y_1	0.55	0.58	1.22	0.66	0.11	0.12	0.66

enhanced over that associated with the formation of the ^{45}Ti and ^{44}Sc nuclei. This result strengthens the assumption that the 56.4-keV γ ray belongs to the γ decay of ^{45}V.

Similar observations are expected for other ^{45}V γ rays, in particular for the γ ray corresponding to the 36.4-keV transition in ^{45}Ti ($\frac{3}{2}^- \to \frac{7}{2}^-$, see Fig. 10). Unfortunately no good estimates are available for the energy of this transition and it might be more promising to search for additional ^{45}V transitions by studying the γ-ray spectrum measured in coincidence with the 56.4-keV γ ray.

IV. γ-x COINCIDENCE MEASUREMENTS

A few of the bound ^{45}V levels are expected to decay strongly to the ground state via the 56.4-keV state. They were searched for by investigating γ-x coincidences. In Fig. 3, three γ-ray spectra observed in the Ge(Li) detector are shown which are in coincidence with the following γ rays measured by the intrinsic Ge detector: (a) the 36.4-keV ^{45}Ti γ ray [$\frac{3}{2}^- \to \frac{7}{2}^-$ (g.s.)], (b) the 39.8-keV ^{45}Ti γ ray [$\frac{5}{2}^- \to \frac{7}{2}^-$ (g.s.)], and (c) the 56.4-keV γ ray. In each case the coincident event is recognized by a time-to-pulse-height converter using a time range of 2 μsec.

As expected[1] from the level scheme of ^{45}Ti (Fig. 10) a strong γ cascade is observed in Fig. 3(a) which originates from the transitions $\frac{7}{2}^+ \to \frac{5}{2}^+ \to \frac{3}{2}^+ \to \frac{3}{2}^- \to \frac{7}{2}^-$ with γ-ray energies of 482.7, 414.4, 292.7, and 36.4 keV, respectively. The crossover 706.9 keV $\frac{5}{2}^+ \to \frac{3}{2}^-$ transition is also seen. However, no such strong γ cascade from the positive-parity states in ^{45}Ti through the $\frac{5}{2}^-$ state is observed in Fig. 3(b). In particular, within the experimental error the $\frac{3}{2}^+ \to \frac{5}{2}^-$ transition with an energy of 289.3 keV is missing; this is in spite of the fact that the 39.8-keV transition has a small conversion coefficient α (in case of pure $M1$, $\alpha = 0.2$), while the 36.4-keV γ ray corresponds to an $E2$ transition with $\alpha = 16$. The absence of the 289.3-keV γ ray indicates an $E1$ transition which is much more strongly inhibited (by about a factor of 1000) than the 292.7-keV γ ray from the $\frac{3}{2}^+ \to \frac{3}{2}^-$ transition and those usually observed in ^{45}Ti. This is shown in Table II where the reduced transition probabilities $B(E1)$ are compared with the single-particle strengths for a number of $E1$ transitions in ^{45}Ti. The strong inhibition of the $\frac{3}{2}^+ \to \frac{5}{2}^-$ transition also explains the absence of the 482.7-keV and 414.4-keV γ rays in Fig. 3(b). However, the crossover $\frac{5}{2}^+ \to \frac{5}{2}^-$, not yet reported, is observed with an energy of 703.6 keV; this branch is strongly enhanced in comparison with the $\frac{5}{2}^+ \to \frac{3}{2}^-$ transition of 706.9-keV energy due to the large difference in conversion coefficients of the 39.8-keV and 36.4-keV transitions. The same enhancement occurs for the 655.9-keV γ ray which appears via the decay $\frac{9}{2}^+ \to \frac{7}{2}^+ \to \frac{5}{2}^- \to \frac{7}{2}^-$. The $\frac{7}{2}^+ \to \frac{5}{2}^-$ transition with its energy of 1186.6 keV is not shown in Fig. 3(b) but is presented later in Fig. 6(c).

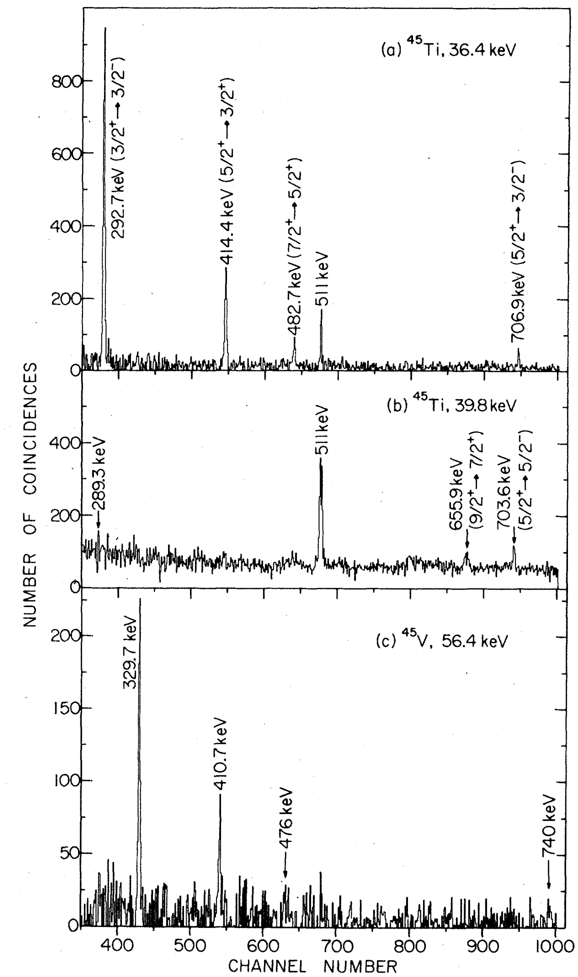

FIG. 3. γ-ray spectra measured in the Ge(Li) detector in coincidence with (a) the 36.4-keV ^{45}Ti, (b) the 39.8-keV ^{45}Ti, and (c) the 56.4-keV ^{45}V γ rays. The low-energy γ rays were measured with the intrinsic Ge detector. The spectra were produced in the bombardment of ^{40}Ca with a 15-MeV ^{7}Li beam. Coincidences were accepted in the time range of 2 μsec. The energies indicated are those obtained by careful calibration with known γ-ray sources.

The γ rays which are in coincidence with the 56.4-keV γ rays are shown in Fig. 3(c). This spectrum strongly resembles that of Fig. 3(a) suggesting that the 56.4-keV γ ray does not correspond to the $\frac{5}{2}^- \to \frac{7}{2}^-$ transition as assumed earlier but to the $\frac{3}{2}^- \to \frac{7}{2}^-$ decay. Fortunately one should be able to distinguish uniquely between these two

TABLE II. The inhibition of some $E1$ transitions in ^{45}Ti. [a]

Initial spin	E_x	$T_{1/2}$	Final spin	Branch %	$_pT_{1/2}$ partial	E_γ keV	$B(E1)$ [b] $e^2\,fm^2$	$\frac{B(E1)}{B(E1)_{W.U.}}$ [c]
$\frac{7}{2}^+$	1226.9	2.8 psec	$\frac{7}{2}^-$	5.1	54.9 psec	1226.9 [d]	4.3×10^{-6}	5.2×10^{-6}
			$\frac{5}{2}^-$	5.7	49.1 psec	1186.4	5.3×10^{-6}	6.5×10^{-6}
$\frac{5}{2}^+$	743.5	10.5 psec	$\frac{3}{2}^-$	8	131.3 psec	706.9	9.4×10^{-6}	1.1×10^{-5}
$\frac{3}{2}^+$	329.1	1.1 nsec	$\frac{5}{2}^-$	$\lesssim0.1$ [e]	$\gtrsim1.1$ sec	289.3	$\lesssim1.1\times10^{-8}$	$\lesssim1.1\times10^{-8}$
			$\frac{3}{2}^-$	100	1.1 nsec	292.7	1.6×10^{-5}	2.0×10^{-5}

[a] Half-lives and branching ratios are taken from Ref. 1.

[b] In order to make the comparison with the single-particle strength $B(E1)_{W.U.}$, the $B(E1)$ values are quoted for the $J_> \to J_<$ transition, where $J_>$ and $J_<$ stands for the larger and smaller spin and $(2J_>+1)B(E1)_{J_>\to J_<} = (2J_<+1)B(E1)_{J_<\to J_>}$ $B(E1) = 0.629\ln 2/{_pT_{1/2}}E^3$ with $_pT_{1/2}$, the partial half-life, in fsec and E in MeV.

[c] The single particle strength is given by $B(E1)_{W.U.} = (1/4\pi)(\frac{3}{4})^2(1.2A^{1/3})^2 = 0.82\ e^2\,fm^2$.

[d] This weak transition is not shown in Fig. 10.

[e] Present work.

transitions by measuring the lifetime of the observed 56.4-keV transition.

V. LIFETIME MEASUREMENTS

The predicted lifetimes of the ^{45}V 56.4-keV γ ray for the two possible transitions $\frac{3}{2}^- \to \frac{7}{2}^-$ and $\frac{5}{2}^- \to \frac{7}{2}^-$ are shown in Table III, Col. 4. They were calculated by using the known lifetimes of the corresponding transition in ^{45}Ti and assuming only pure $E2$ and $M1$ radiation. For the $M1$ transition the reduced transition probability is taken to be the same in ^{45}Ti and ^{45}V. Hence the predicted mean lifetime τ for the $\frac{5}{2}^- \to \frac{7}{2}^-$ transition in ^{45}V equals 6.8 nsec (see Table III). However, since the effective charge of a proton, $1+\delta_p$, is larger than that of a neutron, δ_n, it is expected that for corresponding decays $B(E2)_{^{45}V} > B(E2)_{^{45}Ti}$. In the mirror pair ^{43}Ti-^{43}Sc the ratio $R = B(E2)_{^{43}Ti}/B(E2)_{^{43}Sc}$ had been measured[4] for the $\frac{19}{2}^- \to \frac{15}{2}^-$ decay and equals 1.83. It is assumed that this ratio holds also for the $\frac{3}{2}^- \to \frac{7}{2}^-$ decay in the ^{45}V-^{45}Ti pair leading to a calculated mean lifetime in ^{45}V of 1.04 μsec (see Table III). Since the predicted lifetimes are so different for $M1$ and $E2$ transitions a lifetime measurement should allow us to establish the dominant multipolarity of the 56.4-keV γ ray.

In the first experiment the number of n-x coincidences selecting the 56.4-keV γ ray in the intrin-

TABLE III. Lifetimes in ^{45}V predicted from those observed in ^{45}Ti (pure $E2$ and $M1$ transitions are assumed).

Nucleus +transition	E_γ (keV)	α	Mean lifetime τ (μsec)	$B(E2)_{3/2^-\to7/2^-}$ ($e^2\,fm^4$)	$\frac{B(E2)_{7/2^-\to3/2^-}}{B(E2)_{W.U.}}$ [a]
$\frac{3}{2}^- \to \frac{7}{2}^-$					
^{45}Ti	36.4	16	4.47 [b]	168	8.8
^{45}V	56.4	3.4	1.04 [c]	307.4 [d]	16.1 [d]
$\frac{5}{2}^- \to \frac{7}{2}^-$			τ (nsec)	$B(M1)_{5/2^-\to7/2^-}$ (μ_0^2)	$\frac{B(M1)_{7/2^-\to5/2^-}}{B(M1)_{W.U.}}$ [e]
^{45}Ti	39.8	0.22	17.2 [b]	0.042	0.017
^{45}V	56.4	0.11	6.8 [c]	0.042	0.017

[a] $B(E2)_{W.U.} = 0.0286(1.2A^{1/3})^4(e^2\,fm^4) = 9.5(e^2\,fm^4)$ and $B(E2)_{3/2^-\to7/2^-} = 2B(E2)_{7/2^-\to3/2^-}$.

[b] Reference 7.

[c] Predicted.

[d] $B(E2)_{^{45}V} = 1.83B(E2)_{^{45}Ti}$ (see Ref. 4).

[e] $B(M1)_{W.U.} = 1.79(\mu_0^2)$ and $B(M1)_{5/2^-\to7/2^-} = \frac{4}{3}B(M1)_{7/2^-\to5/2^-}$.

sic Ge detector was measured as a function of the time difference Δt between the start signal in the stilbene crystal and the stop signal in the x-detector. The full range of the time-to-pulse-height converter was set to 500 nsec so that short lifetimes of the order of a few nsec should be observable. A half-life $T_{1/2}=4.2$ nsec or $\tau=6.1$ nsec is observed for the 56.4-keV γ ray as Fig. 4 indicates.

The quality and limitation of the present experiment might perhaps be best tested by measuring a γ decay of similar small energy and lifetime. A suitable candidate is the 39.8-keV ^{45}Ti γ ray with the known lifetime of $\tau=17.2$ nsec or $T_{1/2}=11.9 \pm 0.7$ nsec.[7] Its decay is also plotted in Fig. 4. The measured value of $T_{1/2}=12.3 \pm 0.9$ nsec agrees well with that given in the literature. Also the measured decay curve for the 292.7-keV ^{45}Ti γ ray is shown for comparison. It has a known $T_{1/2}$ value of 1.09 ± 0.01 nsec,[1] while the measured value in Fig. 4 indicates $T_{1/2}=1.2$ nsec. Although the instrumental width of the time-measuring device does not influence the half-life $T_{1/2}=11.9$ nsec of the 39.8-keV γ decay within the experimental error, it might tend to increase the measured value for the 56.4-keV γ decay, and we conclude $T_{1/2} \lesssim 4.2$ nsec or $\tau \lesssim 6.1$ nsec.

The short lifetime $\tau \lesssim 6.1$ nsec very definitely indicates that the 56.4-keV γ ray cannot be the $E2$ $(\frac{3}{2}^- \rightarrow \frac{7}{2}^-)$ transition since for such a transition the $B(E2)$ value should be close to 16.1 $B(E2)_{\text{W.U.}}$ with a lifetime of 1.04 μsec (see Table III). A lifetime of 6.1 nsec, about 163 times smaller, would however result in an unreasonably large transition strength of 2480 $B(E2)_{\text{W.U.}}$. Consequently, one has to assume that the 56.4-keV γ ray corresponds to a predominant $M1$ transition $\frac{5}{2}^- \rightarrow \frac{7}{2}^-$ (g.s.), and the γ decay of the $\frac{3}{2}^-$ state is not yet identified. One expects that it should appear in delayed coincidences and, according to the ^{45}Ti spectrum, in coincidence with the relatively strong γ rays of 329.7-keV and 410.7-keV energy seen in Fig. 3(c).

The search for the long-lived $\frac{3}{2}^-$ state led to the second lifetime experiment. Again the number of γ-x coincidences were measured as a function of time. The γ-detector selected only the 330-keV and 411-keV γ rays and the low-energy γ rays were displayed by the x-detector. The full range of the time-to-pulse-height converter was set to 4 μsec. It became obvious that the 56.4-keV γ ray appeared again in the spectrum of the x-detector but now with delay times much larger than the established short lifetime of $\tau \lesssim 6.1$ nsec. This is shown in Fig. 5 where the number of γ-x coincidences is given as function of time channels. Each time channel represents a time delay of 104 nsec. Although the number of coincidences is small and statistical errors are large, a decay time $\tau=620$ nsec or $T_{1/2}=430 \pm 80$ nsec could be deter-

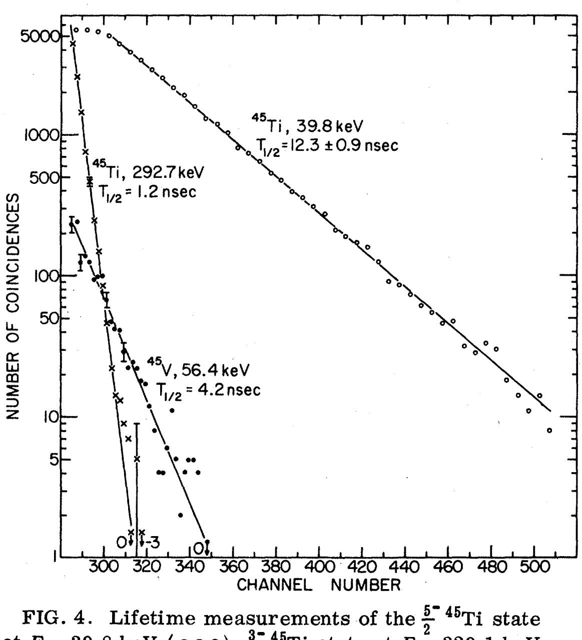

FIG. 4. Lifetime measurements of the $\frac{5}{2}^-$ ^{45}Ti state at $E_x=39.8$ keV (ooo), $\frac{3}{2}^-$ ^{45}Ti state at $E_x=329.1$ keV (×××), and $\frac{5}{2}^-$ ^{45}V state at $E_x=56.4$ (•••). The decays were studied by observing the yields of n-x coincidences as function of time in the bombardment of ^{40}Ca with a 16-MeV ^{7}Li beam. The time dispersion equals 0.526 nsec per channel.

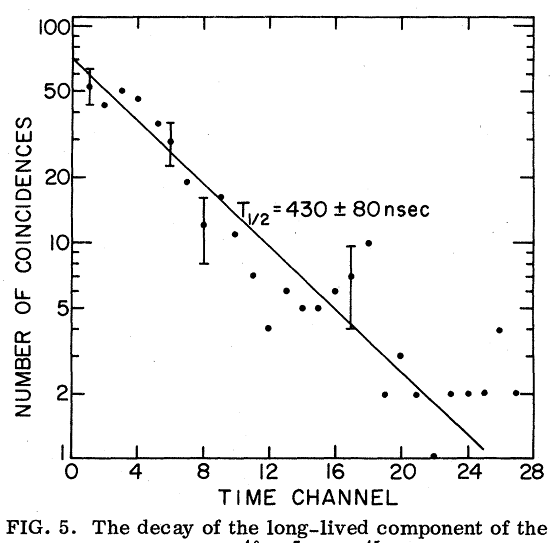

FIG. 5. The decay of the long-lived component of the 56.4-keV γ ray using the ^{40}Ca(^{7}Li, $2n$)^{45}V reaction with a 15-MeV ^{7}Li beam. The yields of the 56.4-keV γ ray in coincidence with the 328.9-keV and 410.7-keV γ rays were added and plotted as function of time with a dispersion of 104 nsec per channel.

mined for the 56.4-keV γ ray. This decay time could also be observed in the n-x coincidences. However, the signal-to-background ratio in these coincidence measurements was appreciably smaller, making the errors even larger.

In conclusion it appears that the 56.4-keV γ ray is associated with two lifetimes. This can be explained by assuming a doublet at an energy of about 56.4 keV. The upper member of the doublet decays to the lower one, and the energy difference between the two members might be observable in a comparison between prompt and delayed coincidences.

VI. PROMPT AND DELAYED COINCIDENCES

A comparison of prompt and delayed γ-x coincidences is shown in Fig. 6. For the two top spectra (a) and (c) the time differences Δt between start and stop pulses were chosen to be $\Delta t = 0 \rightarrow 30$ nsec, representing the prompt coincidences, while the two spectra (b) and (d) at the bottom represent delayed coincidences with $\Delta t = 150 \rightarrow 1720$ nsec. In all cases the γ-ray spectrum of the Ge(Li) detector is presented in coincidence with either the ^{45}V 57-keV γ rays, Figs. 6(a) and 6(b), or with the ^{45}Ti 39-keV γ ray, Figs. 6(c) and 6(d). The latter transition has a lifetime $\tau = 17.2$ nsec and hence the strong coincident 1186.6-keV γ ray (see Fig. 10) is only observable in the prompt coincidence spectrum, Fig. 6(c), while in ^{45}V the 330-keV and, to a lesser degree, the 410.7-keV γ rays are seen in the prompt as well as in the delayed coincidence spectra. So, the two spectra of Figs. 6(a) and 6(b) seem to be the same except for perhaps a slight energy shift of less than 1 keV in the 329.7-keV peak. To investigate this situation in greater detail the measurements were repeated with a much increased energy dispersion in the γ-detector. The result is presented in Fig. 7. It reveals that the 56.4-keV γ ray seen in prompt coincidence is connected with a 329.7-keV γ ray, while in the delayed coincidence a γ ray of only 328.9-keV energy is observed. This shift of 800 eV indicates not only that ^{45}V has a doublet at an excitation energy of about 56.4 keV but that the upper member of this doublet has the long lifetime and the lower one the short lifetime. Hence the $\frac{5}{2}^-$ state is located at 56.4 keV while the $\frac{3}{2}^-$ state has an excitation energy of 57.2 keV, and one observes in Fig. 7 the two transitions $\frac{3}{2}^+ \rightarrow \frac{5}{2}^-$ and $\frac{3}{2}^+ \rightarrow \frac{3}{2}^-$. The comparison with ^{45}Ti [see Fig. 3(a)] suggests that the 410.7-keV γ ray corresponds to the $\frac{5}{2}^+ \rightarrow \frac{3}{2}^+$ transition, and consequently it should not be energy shifted in prompt and delayed coincidences. Indeed no such energy shift was observed. However, for the weak 476-keV and 740-keV γ rays the signal-to-noise ratio is small and the statistical errors large so that our measurements are not good enough to make any statements about possible small energy shifts of these two transitions.

Finally, an attempt has been made to measure the decay of the two members of the doublet. The lower member should be easily observable in the spectrum of the x-detector by measurements in prompt coincidence with either the 329.7-keV or the 410.7-keV γ ray. This is indeed true as seen in Fig. 8(a) where the two spectra are added channel-by-channel and the sum presented. For the upper member of the doublet the spectrum was measured in delayed coincidence with either the 328.9-keV or the 410.7-keV γ ray. Again the two spectra were added and the sum is shown in Fig. 8(b). If both levels of the doublet decay predominantly to the ground state, the spectra of Figs. 8(a) and 8(b) would be expected to exhibit a distinct shift of about five channels similar to the one

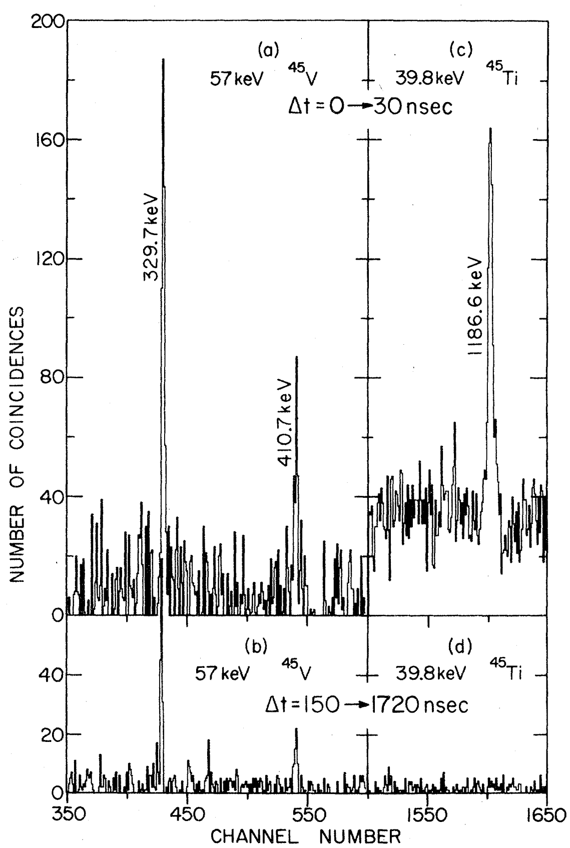

FIG. 6. Prompt and delayed γ-ray spectra measured in coincidence with the ^{45}V γ ray of 56.7 ± 0.8 keV [(a) and (b)] and with the ^{45}Ti γ ray of 39.8-keV energy [(c) and (d)]. The accepted time range is 30 nsec for (a) and (c), and 150–1720 nsec for (b) and (d). The γ-x coincidences were observed in the bombardment of ^{40}Ca with a 15-MeV ^{7}Li beam.

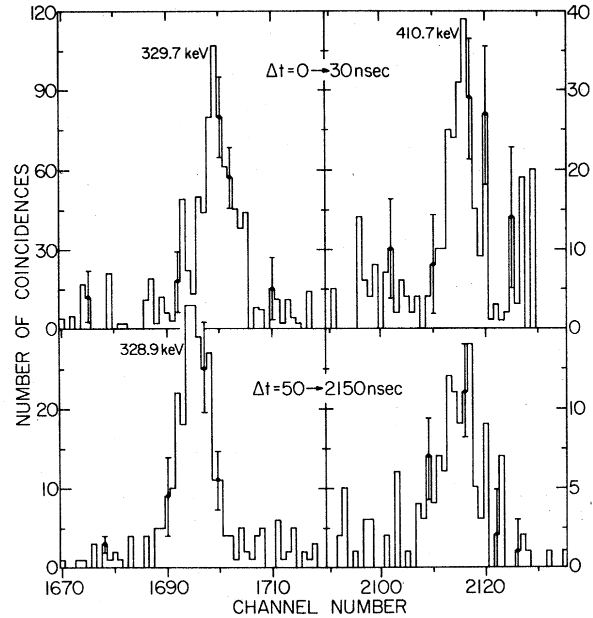

FIG. 7. γ-ray spectra measured in coincidence with the low-energy γ rays of 56.7 ± 0.8 keV. The coincidence spectra were observed in the reaction ^{40}Ca(^{7}Li, $2n$)^{45}V with a 16-MeV ^{7}Li beam. Backgrounds have been subtracted. For the top spectrum the coincidences were accepted within the time range of 30 nsec, for the bottom spectrum the range was 50–2150 nsec. The energy dispersion equals 0.19 keV per channel.

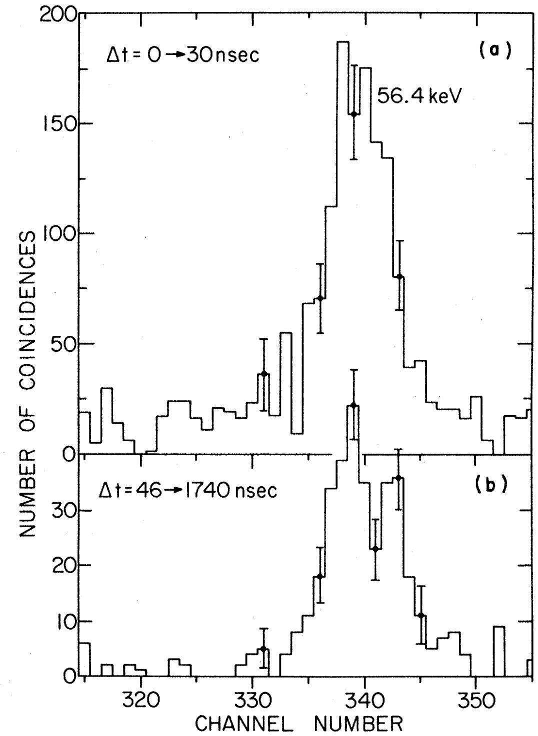

FIG. 8. Low-energy γ-ray spectra obtained in coincidence (a) with the ^{45}V γ rays of 329.7 keV and 410.7 keV, and (b) with the ^{45}V γ rays of 328.9-keV and 410.7-keV energy. The top spectrum represents coincidences within the time range of 30 nsec, the bottom spectrum coincidences within a time range of 46→1740 nsec. The energy dispersion is 0.17 keV per channel. Background has been subtracted. The ^{40}Ca(^{7}Li, $2n$)^{45}V reaction with a 16-MeV ^{7}Li beam was used.

observed for the 329.7-keV and 328.9-keV γ rays in Figs. 7(a) and 7(b). Such a shift is not seen, thus suggesting a strong decay branch of the $\frac{3}{2}^-$ state to the $\frac{5}{2}^-$ state by an 800-eV transition. However, although a distinct energy shift is not observed, the delayed spectrum might consist of a predominant 56.4-keV γ ray and a somewhat weaker γ ray of 57.2-keV energy which is the direct ground-state transition $\frac{3}{2}^- \rightarrow \frac{7}{2}^-$. This question was investigated in more detail with results as shown in Fig. 9. The measured prompt spectrum of Fig. 8(a) is again indicated in Fig. 9(a) by solid points. A smooth curve was fitted through this spectrum which served as a reference peak in the analysis of the measured delayed coincidences. The measured delayed spectrum [Fig. 8(b)] is presented in Figs. 9(b) and 9(c) by solid points. It is fitted with the assumption that it consists of only one γ ray [Fig. 9(b)], while in Fig. 9(c) two γ rays, 800 eV apart, participate. The fitted spectrum is again indicated by the solid curve. It seems that the composite spectrum of Fig. 9(c) fits the measured one quite well, indicating the direct ground-state transition $\frac{3}{2}^- \rightarrow \frac{7}{2}^-$ in addition to the 56.4-keV γ ray. The two decomposed spectra are presented in Fig. 9(d). Although (because of poor statistics) the existence of the direct ground-state transition is somewhat uncertain, a lower limit of ~5 : 1 can be placed on the intensity ratio of the two γ rays. Since they have, according to Table III, α values of 0.11 ($\frac{5}{2}^- - \frac{7}{2}^-$) and 3.4 ($\frac{3}{2}^- \rightarrow \frac{7}{2}^-$), the $\frac{3}{2}^-$ state decays with a probability of at least 55% to the $\frac{5}{2}^-$ state, a transition of 800-eV energy. This transition must be almost completely internally converted; for an $M1$ transition an α value of 2876 has been calculated using the code CATAR.[8]

For an estimate of the partial lifetime of this 800-eV $\frac{3}{2}^- \rightarrow \frac{5}{2}^-$ transition a reasonable assumption might be to use the same reduced transition probability $B(M1)$ as that observed $\frac{5}{2}^- \rightarrow \frac{7}{2}^-$ transition in ^{45}Ti, $B(M1) = 0.042\mu_0^2$ (see Table III). With this value and $\alpha = 2876$ the partial lifetime $\tau_1 = 918$ nsec is obtained. Considering the other possible decay of the $\frac{3}{2}^-$ state, namely $\frac{3}{2}^- \rightarrow \frac{7}{2}^-$, for which the comparison with ^{45}Ti gives an estimated partial lifetime $\tau_2 = 1.04$ μsec (Table III), the total decay of the $\frac{3}{2}^-$ state should occur with a mean lifetime of $\tau_{\text{total}} = 488$ nsec or $T_{1/2} = 333$ nsec. This value

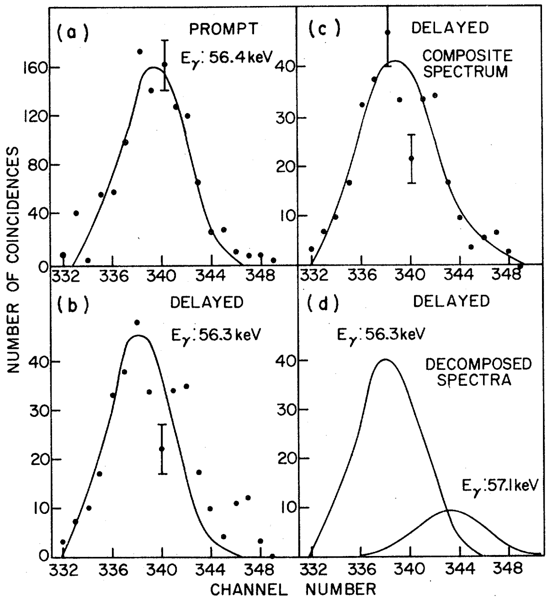

FIG 9. Analysis of the 56.4-keV ^{45}V γ ray obtained in prompt and delayed coincidences as shown in Figs. 8(a) and 8(b). Solid points represent the measurements; in Fig. 9(a) the prompt spectrum of Fig. 8(a) and in Figs. 9(b) and 9(c) the delayed spectrum of Fig. 8(b) are shown. Solid lines in Fig. 9(a) indicate a smooth curve through the measured values which is taken as a reference peak for the analysis of the delayed spectrum. For the latter spectrum the assumptions have been made that it represents first, only one γ ray [Fig. 9(b)], and second, two γ rays 800 eV apart [Fig. 9(c)]. With these assumptions and the reference peak, a spectrum is calculated (solid lines). The two components of the composite spectrum [Fig. 9(c)] are shown in Fig. 9(d). The indicated energies are those obtained for the calculated peaks.

agrees quite well with the measured result of $T_{1/2}$(meas)$=430\pm80$ nsec (see Fig. 5) since one has to keep in mind that the $B(M1)$ and $B(E2)$ values chosen for the calculation are expected to be only approximately right. Furthermore, one can conclude from the predicted τ_1 and τ_2 values that the $\frac{3}{2}^-$ state is expected to decay in the ratio $I(\frac{3}{2}^- \to \frac{5}{2})/I(\frac{3}{2}^- \to \frac{7}{2}^-)$ of about 1 : 1. This value agrees well with 1.2, the estimate obtained above from the decomposition of the measured delayed spectrum [see Figs. 9(b)–9(d)]. Certainly this result indicates that the decay of the $\frac{3}{2}^+$ state in ^{45}V exhibits not only the $\frac{3}{2}^+ \to \frac{3}{2}^-$ transition as seen in ^{45}Ti, but also reveals a comparably strong $\frac{3}{2}^+ \to \frac{5}{2}^-$ transition. The unusually strong inhibition of the latter transition in ^{45}Ti (see Table II) may arise accidentally by contributions from small wave function components.

The measured decay mode of the $\frac{3}{2}^-$ state, its lifetime and its population by the 328.9-keV γ ray

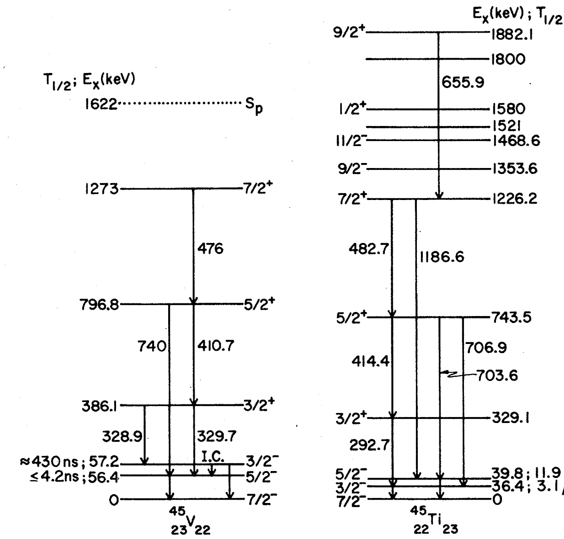

FIG. 10. Level schemes of ^{45}V from the results of the present work, and of ^{45}Ti (Refs. 1 and 7). All γ-ray energies are obtained from careful energy calibrations in the present work. The excitation energies quoted for the different states are derived from those γ-ray transitions which show the smallest energy uncertainty. However, the energies of the states at $E_x = 1353.6$, 1468.6, 1521, 1580, and 1800 keV are taken from Ref. 1.

emitted from the $\frac{3}{2}^+$ state at 386.1 keV helped to determine the level scheme of ^{45}V.

VII. DISCUSSION AND CONCLUSIONS

The results of our γ-ray studies indicate a ^{45}V level scheme which is shown together with that of ^{45}Ti in Fig. 10. For some of the states the spin assignment can be determined independently, as indicated in the discussion below.

A. Quasirotational band

It is known that positive-parity states of f-shell nuclei with a one-hole–many-particle configuration exhibit a quasirotational behavior; their excitation energy shows a smooth dependence on $J(J+1)$ where J is the spin. Examples are given in Fig. 11 for the states $\frac{3}{2}^+$, $\frac{5}{2}^+$, $\frac{7}{2}^+$, and $\frac{9}{2}^+$ in ^{43,45}Ti and ^{43}Sc. The positive-parity states of ^{45}V as determined by the present γ-ray studies follow a similar behavior, thereby confirming for these states the spin assignments given in Fig. 10.

B. Coulomb displacement energies

For a homogeneously charged spherical nucleus the Coulomb displacement energy ΔE_c of $T_{1/2}$ mirror nuclei is expected to be proportional to the charge Z. Since

$$E_{\mathrm{Coul}} = \tfrac{3}{5} Z(Z-1)e^2/R$$

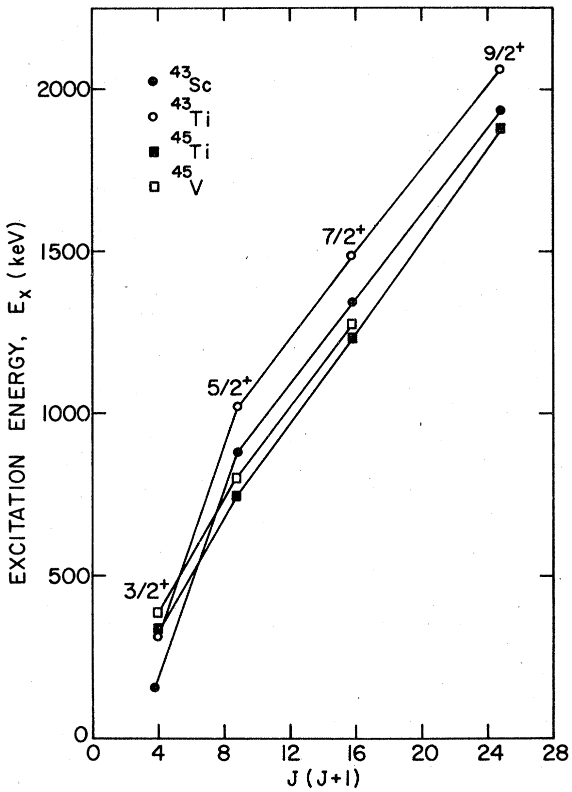

FIG. 11. Excitation energy E_x as function of $J(J+1)$, where J indicates the spin. The symbols represent: ●●● ^{43}Sc (Ref. 9), ○○○ ^{43}Ti (Ref. 10), ■■■ ^{45}Ti (Ref. 1), and □□□ ^{45}V (present work).

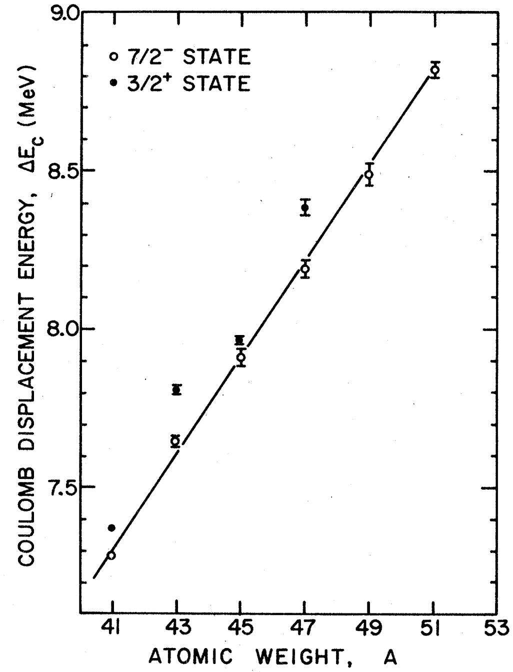

FIG. 12. Coulomb displacement energy ΔE_c as function of the atomic weight A for $T=\frac{1}{2}f_{7/2}$-shell nuclei. The first $\frac{7}{2}^-$ states are indicated by open circles, the first $\frac{3}{2}^+$ states by solid points. The references are for: $A=41$, Ref. 11, 12; $A=43$, Ref. 11, 10; $A=45$, Ref. 11, 1, present work; $A=47$, Ref. 11, 13, 14; $A=49$, Ref. 11, 13; $A=51$, Ref. 11, 13.

it follows that

$$\Delta E_c(\text{keV}) = M_{Z_>} - M_{Z_<} + 782.4 = \tfrac{6}{5}e^2 Z_</R,$$

where M equals the mass (in keV), $Z_>$ and $Z_<$ indicate the larger and smaller charge of the two mirror nuclei, R is the radius of the nucleus, and 782.4 is the np mass difference in keV. Since only a small range of the atomic weight A is considered and $A=2Z_<+1$ for $T=\frac{1}{2}$ mirror nuclei, the value ΔE_c should be nearly proportional to A. Indeed this dependence is rather well established for the f-shell nuclei as shown in Fig. 12. The open circles indicate the values for the first $\frac{7}{2}^-$ state. The deviations from a straight line are small. The largest one of about 40 keV, observed for $A=43$, might be due to the pairing effect which is seen in lower-shell nuclei (see, for example, Ref. 3). Consequently one can regard the observed ΔE_c value as an independent indicator to determine the spin of the first $\frac{7}{2}^-$ state in case of low-level density. The ^{45}Ti–^{45}V pair is also included in Fig. 12 using the mass values of Ref. 11 for both nuclei and assuming that the $\frac{7}{2}^-$ state is the ground state in ^{45}V. One recognizes that the regularity in the ΔE_c dependence might perhaps permit the $\frac{7}{2}^-$ state to be located at an excitation energy of 56 keV; the ΔE_c value would be 7962 keV. However, the state at 386 keV (see Fig. 10) with its ΔE_c value of 8294 keV is excluded. A similar A dependence is observed in Fig. 12 for the $\frac{3}{2}^+$ states although some fluctuations in ΔE_c values are revealed. The ΔE_c value for $A=45$ using the excitation energy of 386 keV for the $\frac{3}{2}^+$ state in ^{45}V is indicated in Fig. 12. The value fits with those of the neighboring mirror pairs. In fact, a shift of the $\frac{3}{2}^+$ state to the nearest neighboring states with excitation energies of either 796 keV or 56 keV (see Fig. 10) results in an ΔE_c value of either 8374 keV or 7634 keV; both values are far removed from the trend observed in neighboring nuclei. We take this as another confirmation that the $\frac{3}{2}^+$ state is located at $E_x=386.1$ keV. Consequently the A dependence of the Coulomb displacement energy restricts the $\frac{7}{2}^-$ spin assignment to either the ground state or to one member of the 57-keV doublet and the $\frac{3}{2}^+$ spin to the level at $E_x=386.1$ keV. However, the spin sequence of the first four states (Fig. 10) is uniquely determined by the observed γ decay and the lifetime measurements.

A more detailed discussion of the Coulomb displacement energies in $T=\frac{1}{2}$ nuclei will be presented.[2]

ACKNOWLEDGMENTS

The authors are grateful to K. E. Rehm who participated in the beginning of the present work. We are also indebted to R. D. Lawson and J. P. Schiffer for many helpful discussions. We would like to thank the tandem operating staff for their cooperation and G. E. Thomas for his efforts to provide us with the necessary targets. Wayne Bentley of Michigan State University kindly performed calculations of internal conversion coefficients for us. One of us (G.H.) wishes to thank the Argonne National Laboratory for support through a Faculty Research Participation Grant.

---

*Present address: Phys. Res. Lab., Mass. General Hospital, Boston, Mass. 02114.

[1]J. R. Beene, Nucl. Data Sheets 22, 1 (1977).
[2]L. Meyer-Schützmeister, G. Hardie, S. A. Gronemeyer, and A. J. Elwyn (unpublished).
[3]D. Mueller, E. Kashy, W. Benenson, and H. Nann, Phys. Rev. C 12, 51 (1975).
[4]L. Meyer-Schützmeister, A. J. Elwyn, K. E. Rehm, and G. Hardie, Phys. Rev. C 4, 1299 (1978).
[5]B. A. Brown and R. Sherr, Nucl. Phys. A322, 61 (1979).
[6]M. Blann and F. Plasil, University of Rochester Report No. UR-NSL-181, 1978 (unpublished).
[7]F. J. Lynch, K. -E. Nysten, R. E. Holland, and R. D. Lawson, Phys. Lett. 32B, 38 (1970).
[8]H. C. Pauli and U. Raft, Comput. Phys. Commun. 1, 392 (1975).
[9]G. C. Ball, J. S. Forster, F. Ingebretsen, and C. F. Monahan, Can. J. Phys. 48, 2735 (1970).
[10]L. Meyer-Schützmeister, A. J. Elwyn, S. A. Gronemeyer, G. Hardie, R. E. Holland, and K. E. Rehm, Phys. Rev. C 18, 1148 (1978).
[11]A. H. Wapstra and K. Bos, At. Data Nucl. Data Tables 19, 175 (1977).
[12]P. M. Endt and C. van der Leun, Nucl. Phys. A310, 1 (1978).
[13]D. Mueller, E. Kashy, and W. Benenson, Michigan State University Report No. MSUCL 233, 1977.
[14]G. Hardie *et al.* (unpublished).